Continuous adsorption in food industry

The recovery of sinapic acid from rapeseed meal extract

Moreno-González, Mónica; Keulen, Daphne; Gomis-Fons, Joaquín; Gomez, Gustavo Lopez; Nilsson, Bernt; Ottens, Marcel

DOI
10.1016/j.seppur.2020.117403

Publication date
2021

Document Version
Final published version

Published in
Separation and Purification Technology

Separation and Purification Technology 254 (2021) 117403

Contents lists available at ScienceDirect

Separation and Purification Technology

journal homepage: www.elsevier.com/locate/seppur

Continuous adsorption in food industry: The recovery of sinapic acid from rapeseed meal extract

Mónica Moreno-González[a], Daphne Keulen[a], Joaquín Gomis-Fons[b], Gustavo Lopez Gomez[a], Bernt Nilsson[b], Marcel Ottens[a,*]

[a] Department of Biotechnology, Delft University of Technology, van der Maasweg 9, 2629 HZ Delft, the Netherlands
[b] Department of Chemical Engineering, Lund University, 22100 Lund, Sweden

ARTICLE INFO

Keywords:
Adsorption
Batch
Semi-continuous
CaptureSMB
Model based optimization
Polyphenols
Industrial side stream valorization

ABSTRACT

Efficient recovery and utilization of valuable components from industrial food side streams is a main driver towards a circular economy. Among different available purification techniques, adsorption can effectively recover these components. However, the conventional batch mode of operation can limit its applicability in food processes due to limited efficiency. This work compares conventional batch packed bed adsorption with semi-continuous adsorption (so-called CaptureSMB) for the recovery of sinapic acid at industrial scale, using a food grade resin Amberlite™ FPX66. A mathematical mechanistic model able to describe semi-continuous operation is successfully validated and used to identify optimum operating parameters to maximize productivity and resin capacity utilization in batch and semi-continuous operating modes. The results indicate that CaptureSMB outperforms batch operation, increasing productivity from 5.18 g/L/h to 10.3 g/L/h for a given yield (> 97%). A resin capacity utilization (RU) of around 70% is observed in both operating modes when productivity is maximized. A 92% RU can be accomplished for a given yield using the CaptureSMB process at a productivity of 7.0 g/L/h, higher than for conventional batch operation. The use of semi-continuous adsorption operation in food industry contributes to more efficient processes at reduced purification costs.

1. Introduction

Voluminous side streams are generated during the supply chain of food products. These side streams are complex mixtures that often contain valuable products that can be valorized, via recovery and reuse in the food chain [1]. For instance, proteins can be recovered from agricultural residues such as oilseed meals [2–4], cereals are sources of complex carbohydrates such as hemicellulose, arabinoxylans and glucans while fruits and vegetables are sources of polyphenols [1]. Valorization and recovery of these compounds have been conducted using well established methodologies, like the universal 5 step methodology suggested by Galanakis (2012), with the application of conventional techniques such as precipitation, filtration, adsorption and extraction, amongst others [1]. Recovering these valuable products can contribute to a more circular economy by reducing waste generation and maximizing resource potential. In addition, the improved efficiency could lead to cost reduction.

Among different separation techniques, adsorption is a powerful technology able to separate complex mixtures at mild operating conditions, often desired in food processes. Large scale batch adsorption processes have been implemented for sugar and isomers separation, fractionation of amino acids and proteins, purification of penicillin and enzyme production [5]. However, some disadvantages of batch adsorption are: high buffer consumption, low productivity and high stationary phase cost, as not all the adsorbent in the column is efficiently used.

The application of continuous or semi-continuous adsorption can overcome the limitations of batch operation. Improved capacity utilization, which subsequently results in reduced buffer consumption, shorter processing times and cost savings can be accomplished [6]. The usage of connecting columns (smaller packed beds) in series and a flexible valve system to switch the inlets (feed, wash and eluting buffers) at the right time (simulating countercurrent movement) allows a more efficient operation.

Continuous chromatography has been successfully implemented in the (petro)chemical field mainly with variants of simulated moving bed (SMB) [7–10] technology. The Hypersorption process [11], purification of L-Lysine from Calgon Carbon, Vitamin C production from Sep Tor Technologies and the different applications of the UOP Sorbex process (Parex, Molex, Olex) [12] are some examples. The applied flow rates

* Corresponding author at: Department of Biotechnology, Delft University of Technology, van der Maasweg 9, 2629 HZ Delft, the Netherlands.
E-mail address: M.Ottens@tudelft.nl (M. Ottens).

https://doi.org/10.1016/j.seppur.2020.117403
Received 18 May 2020; Received in revised form 8 July 2020; Accepted 15 July 2020
Available online 21 July 2020

could go up to 150 m^3/h and these SMB systems are typically operated with more than four columns having product capacities from 30 to 400 kton/a [13]. The pharmaceutical sector has found SMB applications in chiral separation [14] at a significant lower production scale, up to 10 ton/a. The biopharmaceutical sector has increased its interests in continuous operation and new developments in semi-continuous systems have been introduced such as periodic countercurrent chromatography (PCC) [15,16], the sequential multicolumn chromatography (Varicol) from Novasep [17,18], the multicolumn countercurrent solvent gradient purification (MCSGP) [19,20], mainly used for monoclonal antibody purification. While in the food sector, SMB technology has been investigated in different areas such as desugarization and fractionation of molasses, oligosaccharides and organic acid separations, dairy streams protein purification, peptides isolation from hydrolysates [21–26] and separation of fructose-glucose [27–29] and the Sarex process [13]. These applications show the potential of using continuous chromatography for purification of more complex streams such as food by-products for the recovery of nutraceuticals (polyphenols) or natural food ingredients, which can also be aligned with the continuous operation of food processes.

In terms of equipment complexity, systems with few columns are preferred, as control and number of devices needed for operation (valves, pumps, pipes and detectors) increase with the number of columns [30]. The recently developed twin column system, CaptureSMB (2-PCC system), proposed by Angarita et al. (2015) has been successfully implemented for the capture step of monoclonal antibodies, showing comparable or better performance than systems with higher number of columns [31,32], which makes it an interesting system with potential application in food industry.

This work compares the performance of the semi-continuous system CaptureSMB with conventional batch operation (packed bed) for the recovery of sinapic acid (a nutraceutical) from rapeseed meal extract (food by-product). The study begins with the adaptation of a previously developed one-column adsorption model [33] to a two-column system, CaptureSMB, followed by its experimental validation at lab scale. Both models (batch and semi-continuous) were later used to find optimum operating parameters to maximize productivity and resin capacity utilization at industrial scale (up to 118 m^3/h). The use of modelling allows the fair comparison of both processes, as the same constraints could be established. Additionally, it minimizes the number of pilot trials. The methodology used in this work can be used as a guide for other food products that involve an adsorption step, where pilot or industrial scale experimentation are not possible.

2. Case study

Rapeseed meal contains mainly crude proteins (40%), crude fibers (12%) and nitrogen-free extract fractions (34%) [34]. When processing the rapeseed meal to acquire the proteins, it is important to remove phytic acid and phenolic content to prevent nutritional value lost. However, phenolic compounds are valuable compounds that can be recovered. Particularly, sinapic acid, major phenolic compound in rapeseed meal, presents antioxidant, antimicrobial, anti-inflammatory activities [35]. Therefore, sinapic acid has potential applications in food, cosmetic and pharmaceutical products. Previous studies have demonstrated that sinapic acid is selectively captured using the polymeric resins Amberlite™ FPX66, while phytic acid, glucose and glucosinolates (impurities) poorly interact with the adsorbent [33].

For industrial applications, a column of 1 m internal diameter and column height between 3 and 12 m was assumed to evaluate the optimization of two adsorptive operating modes. The two adsorption configurations evaluated in this study were: 1) batch operation with packed bed and 2) semi-continuous operation with CaptureSMB.

In both configurations, elution and regeneration phases were assumed to be the same and consisted of washing with 2 column volumes (CV) of water, elution and regeneration with 8 CV of 70% w/w ethanol/water and re-equilibration with 5 CV of citrate-phosphate buffer at pH 6.

3. Materials and methods

3.1. Theory: Adsorption column model

The equilibrium-transport-dispersive chromatography model in combination with the liquid-film linear driving force approximation is used to describe the dynamic adsorption of one column, as described in Eq. (1)

$$\frac{\partial C_i}{\partial t} + F\frac{\partial q_i}{\partial t} + v\frac{\partial C_i}{\partial z} = D_L\frac{\partial^2 C_i}{\partial z^2} \tag{1}$$

where C_i represents the bulk liquid concentration (g/L) of component i, v is the interstitial velocity of the mobile phase (m/s) defined as superficial velocity divided by the bed porosity (u/ε_b), q_i is the stationary phase concentration of component i (g/L_R), F is the phase ratio defined as $F = (1 - \varepsilon_b)/\varepsilon_b$, where ε_b is the bed porosity, and D_L is the axial dispersion coefficient (m^2/s). The solid stationary phase concentration term $\frac{\partial q}{\partial t}$ is defined according to Eq. (2). The lumped kinetic model (LKM) was used for column modelling. This model assumes that the mobile phase concentration in the pores and between the particles is the same [36], therefore a separate mass balance for the pore is not required.

$$\frac{\partial q_i}{\partial t} = k_{ov,i}(C_i - C^*_{eq,i}) \tag{2}$$

The LKM lumps the internal and external mass transfer resistances into an overall mass transfer coefficient k_{ov}(1/s) as defined in Eq. (3).

$$\frac{1}{k_{ov,i}} = \frac{d_p}{6 * k_f} + \frac{d_p^2}{60 * \varepsilon_p * D_p} \tag{3}$$

where d_p is the particle diameter (m), k_f is the film mass transfer coefficient (m/s), $\varepsilon_p$is the intraparticle porosity and D_p is the pore diffusivity (m^2/s). D_L and other relevant model parameters were calculated using different mass transfer correlations as described in Moreno-González et al. (2020). The equilibrium concentration $C^*_{eq,i}$, is calculated using the Langmuir isotherm (Eq. (4))

$$q_i = \frac{H_i C^*_{eq,i}}{1 + \frac{H_i}{q_{max,i}} C^*_{eq,i}} \tag{4}$$

where q_i is the adsorption capacity (g/L_R), H_i is the isotherm slope ($H_i = q_{max,i}K_i$), $q_{max,i}$ is the maximum adsorption capacity (g/L_R), K_i is the equilibrium constant (L/g) of the species being adsorbed [37]. In order to include the isotherm slope dependency on the modifier concentration a power function was used as described elsewhere [33,38].

In the adsorption model an initial condition (at $t = 0$) and boundary conditions for the inlet and outlet are required. The assumption for the initial condition is that the column is not preloaded (free of components $C_i(t = 0) = 0$; $q_i(t = 0) = 0$). The in- and outlet conditions are described by Danckwerts boundary conditions for dispersive systems (Eqs. (5) and (6)):

$$\text{Inlet:} \quad (t, x = 0) = C_{inlet,i} - \frac{D_{L,i}}{v}\frac{\partial C_i(t, x = 0)}{\partial x} \tag{5}$$

$$\text{Outlet:} \quad \frac{\partial C_i(t, x = L)}{\partial x} = 0 \tag{6}$$

3.1.1. CaptureSMB process

The concept of periodic countercurrent chromatography (PCC) is to switch the connection between columns during the different steps (e.g. loading, washing, elution and regeneration) of the chromatography process. In this study the 2-PCC, patented by ChromaCon as CaptureSMB, is studied [39]. The operation mode depends on the

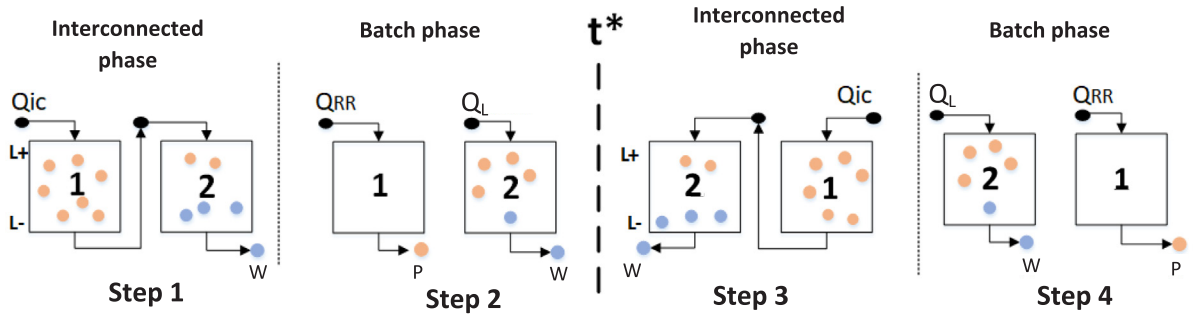

Fig. 1. Schematic presentation of a CaptureSMB system.

breakthrough moments for the applied flow rates during the interconnected and disconnected phase. An overview of the process is shown in Fig. 1, separated in four steps.

There are two different phases in one-time switch (t^*), indicated in Fig. 1 as interconnected and batch phase. First the columns are connected in series (i.e. interconnected time), the first column is loaded up to a certain percentage of dynamic binding capacity (DBC), step 1 and the breakthrough is captured by the second column. Subsequently (step 2) the first column is washed, eluted and regenerated to obtain the product while the second column is loaded with the feed. Once the first column is regenerated, the columns are connected again (time switch, $t^* = t_b + t_{ic}$), and switch positions (column 2 becomes column 1). Step 3 is performed; the columns are connected in series and subsequently disconnected. In Step 4, the product is recovered from column 1 while column 2 is loaded with the feed. A cycle is completed when two-times switches are completed and the columns return to their starting positions (steps 1 to 4). In this work column 1 is referred as the first column in the column interconnection.

The interconnected phase has a certain duration (interconnected time, t_{ic}) and it is performed at an interconnected flow rate Q_{ic} (m^3/h). The time needed in the batch phase is defined by the elution/regeneration protocol. While the first column performs the task of recovering the bound product and regenerating the column at a flow rate Q_{rr}, the second column is loaded with the feed at a flow rate Q_L. The parameters to be optimized in the CaptureSMB process are the interconnected and loading flow rates (Q_{ic} and Q_L) and the interconnected time (t_{ic}) [32]. In this work, superficial velocities were used instead of flow rates, as the flow rate is a function of this velocity and the cross-sectional area of the columns.

Even though there is a continuous input of feed using the CaptureSMB process, the operation is semi-continuous due to discontinuous collection of the product.

3.1.2. Capture SMB model

Adapting the adsorption model of one column to a CaptureSMB configuration results in the simulation of the transport-dispersive model [36] for two columns connected, where the output of one column is the input of the next one. The main changes and/or additions compared to batch chromatography are: different boundary conditions for each column, multiple flow rates, time switches, timespan and operating variables.

In the CaptureSMB model the balance of each solute (i) transported through each column (j) is solved [9] (Eq. (1)).

The connecting nodes between the columns (black nodes in Fig. 1) are set-up according to the specific process configuration, and they determine the boundary conditions for each column. Column switching was implemented by a periodic movement of the concentration vector. The concentration vector is moved at the end of the switching interval by a step size of one column length against the direction of fluid flow. The duration of one cycle is equal to the amount of columns times the time-span of one time-switch ($t_{cycle} = 2\ t^*$). Moreover, the total time depends on the amount of cycles set and after multiple time switches a cyclic steady state is reached, which means that the same elution profile is repeated every cycle. The initial conditions at ($t = 0$) assume that the columns are not preloaded with the product (start-up phase) and this is subsequently altered after every switch. The new initial conditions are equal to the conditions at the time switch (Eqs. (7) and (8))

$$C_{0,i} = C_i(t = n{\cdot}t^*) \tag{7}$$

$$q_{0,i} = q_i(t = n{\cdot}t^*) \tag{8}$$

where t^* denotes the time switch and n the number of switches set. The main assumptions made for the continuous model are that the columns are identical and the dead volume between the columns is neglected.

The boundary conditions are different for each column and changes from interconnected to batch phase in one-time switch. The beginning and end of the column in Fig. 1 is denoted by L^+ and L^-. The boundary conditions for the interconnected phase are expressed in Eqs. (9) and (10).

$$C_i(t, L^+(columnI)) = C_{feed,i} \tag{9}$$

$$C_i(t, L^+(columnII)) = C_i(t, L^-(columnI)) \tag{10}$$

Since the two columns are connected in series, the inlet of the second column is equal to the outlet of the first column.

The boundary conditions for the batch phase are shown in Eqs. (11) and (12).

$$C_i(t, L^+(columnI)) = 0 \tag{11}$$

$$C_i(t, L^+(columnII)) = C_{feed,i} \tag{12}$$

The first column in the batch phase undergoes elution and regeneration, therefore, the inlet feed concentration is zero, while the second column is loaded with the feed at a flow rate (Q_L).

The dynamic model is a function of time and space (Eq. (1)) and can be described by a partial differential equation (PDE), while ordinary differential equations (ODEs) only include one variable. The Method of Lines was applied for the spatial discretization in order to transfer the PDE into a set of ordinary differential equations (ODEs) with respect to time. The system of ODEs was numerically solved using an implicit solver (*ode15s*) for stiff differential equations in MATLAB R2017b software.

3.1.3. Batch and continuous process optimization

Batch and continuous operations were optimized for large-scale implementation in food industry, where column dimensions are significantly larger than the ones used by pharmaceutical companies. Maximum productivity is important for food industry as voluminous streams are usually generated. The following optimization problems were defined:

Batch optimization

$$\text{Optimization function} \quad \max Prod(u_{batch}) \tag{13}$$

Subject to $C_i(t = t_{ads}, z = L_c) \leq 0.04 C_{feed,i}$ (14)

$Yield \geq 97\%$

$L_c = 3m, 6m \ and \ 12m$

$0 < t_{ads}; 2.45 < u_{batch} \leq 205 m/h$

where u_{batch} is the superficial velocity and t_{ads} is the adsorption time. Velocity was varied based on the maximum allowed pressure drop, indicated by the resin supplier (Dow Chemicals).

CaptureSMB optimization

Optimization function $\max Prod(u_{ic}, u_b, t_{ic})$ (15)

Subject to $Yield \geq 97\%$ (16)

$L_c = 3m, 6m \ and \ 12m$

$0 < t_{ic}; \quad 2.45 < u_{ic} \leq 60 m/h$ at $L_c = 3m$;

$2.45 < u_{ic} \leq 110 m/h$ at $L_c = 6m$

$2.45 < u_{ic} \leq 205 m/h$ at $L_c = 12m$

$0 < u_b \leq u_{ic}$

Column length was varied, as experiments showed that lowering the bed height increases the productivity performance of the CaptureSMB process when comparing to batch.

3.2. CaptureSMB adsorption experiments

3.2.1. Resin preparation and column characteristics.

Following resin supplier recommendations, resin FPX66 was washed with water prior to use, to remove chlorine and sodium carbonate salts. Water excess was removed using a glass filter under vacuum and the resin was contacted with ethanol for 30 min. A second washing step was performed to remove ethanol and re-suspend the resin in water prior to column packing.

CaptureSMB process requires two identical columns for operation. A known amount of pre-treated resin FPX66 (2.5 g per column) was placed in two adjustable height Omnifit glass columns (1 cm inner diameter and 15 cm height). The volume of each column was 3.5 mL (4.5 cm column height). Trace pulse experiments with NaCl were done to determine bed porosity corresponding to 0.32 and intraparticle porosity was obtained using the difference between wet and dry weight of the resin which corresponds to a value of 0.56. Resin characteristics can be found in Section 3.3.

3.2.2. Equipment set up

Experiments were performed using an Äkta Avant coupled with the operating system Unicorn 7, provided by GE Healthcare Life Sciences (Uppsala, Sweden). The system configuration is shown in Fig. 2. The implementation of three versatile valves (VV1, VV2 and VV3 in Fig. 2) made it possible to switch between phases. In particular, versatile valve 1 is used to choose between batch and interconnected step, and versatile valves 2 and 3 are used to choose the column to be loaded first, that is, to determine the specific process step. The outlet valve is used to fractionate the breakthrough of the column being loaded during the batch step and the breakthrough of the second column during the interconnected step. The collection of the product pool was carried out with a sample valve used as a second outlet valve, with seven different outlets.

The process was monitored using two UV detectors, a U9-M monitor able to measure up to three wavelengths, equipped with a U9-D UV detector (GE Healthcare Life Sciences, Uppsala, Sweden), the second detector is a U9-L able to measure only one wavelength (280 nm). pH and conductivity were monitored using a V9-pH and a C9 conductivity monitor respectively (GE Healthcare Life Sciences, Uppsala, Sweden). In addition, fractions were collected during the whole process run.

In order to adapt the Äkta Avant system to run a complex process like the CaptureSMB, the research software **Orbit**, developed at Lund University (Sweden), was used. Orbit controller is a program developed in Python that enables the execution of chromatography processes through scripting. Orbit executes its commands through Unicorn via OPC (Object Linking and Embedding for Process Control), i.e., it sends instructions sequentially at different times, and Unicorn executes them. Orbit has been successfully adapted to work in Äkta Pure (with Unicorn 7) [40,41] with column sequences for the purification of biopharmaceuticals. Additionally, it has been adapted to run a 3-column periodic countercurrent chromatography (PCC) process in Äkta Pure [42]. In this case, the scheduling of the CaptureSMB process determines the times at which Orbit sends every instruction to Unicorn.

3.2.3. CaptureSMB run

Initial determination of CaptureSMB operating parameters were done following the methodology described by Angarita et al. [31] and using the simulation of sinapic acid breakthrough curves on FPX66, as previous study showed that the dynamic column model is in good agreement with experimental results [33].

Batch time (t_b) is a function of the elution protocol, which was defined based on the dynamic column model and experiments presented by Moreno-González et al. [33]. The process was run for four cycles. CaptureSMB operating parameters are shown in Table 1. As suggested by Angarita et al. [33], a start-up phase was implemented in order to achieve steady state operation since the second switch. Elution and regeneration protocols are described in Section 2 Case study of this work.

The above parameters were used in the lab scale CaptureSMB process and were later optimized for industrial scale application as described in Section 3.1.3.

UV, pH and conductivity detectors were used to monitor breakthrough of column 1 while breakthrough of column 2 was fractionated (2 mL per fraction) and analyzed for sinapic acid concentration by UHPLC (3.5 Analytical methods). In addition, during step 4 of the last cycle (in the process shut-down), it was decided to continue loading the column up to interconnected time. The outlet was fractionated to verify the product breakthrough in column 1.

3.3. Chemicals

All chemicals were analytical grade: Sodium phosphate, dibasic, 12-hydrate (≥99%) and citric acid (≥99%) were purchased from J.T. Baker, Denmark. Glucose anhydrous for biochemistry and Ethanol: Emsure absolute for analysis were purchased from Merck. Sinapic acid (≥99%), acetonitrile (HPLC grade) formic acid (≥99%) and food grade macroporous resin Amberlite™ FPX66 were purchased from Sigma-Aldrich, Zwijndrecht, The Netherlands. Resin characteristics can be found in Table 2.

3.4. Buffer solutions

Disodium phosphate. Na_2HPO_4, (0.2 M) and citric acid (0.1 M) solutions were prepared using MilliQ water and dissolving the corresponding amount of each chemical. Citrate-phosphate buffer at pH 6 was prepared following the method from McIlvaine [43], the used ratio corresponds to 64.8:35.2 (Na_2HPO_4 mL/Citric acid mL).

Mimicked plant-based extract was prepared by dissolving sinapic acid and glucose in citrate-phosphate buffer at pH 6. The corresponding concentrations were 1.2 g/L sinapic acid and 8 g/L glucose. The selected concentrations are similar to the concentrations of the aqueous extract from rapeseed meal.

All buffer and solutions were filtered previous to use with disposable filters of 0.45 μm pore size.

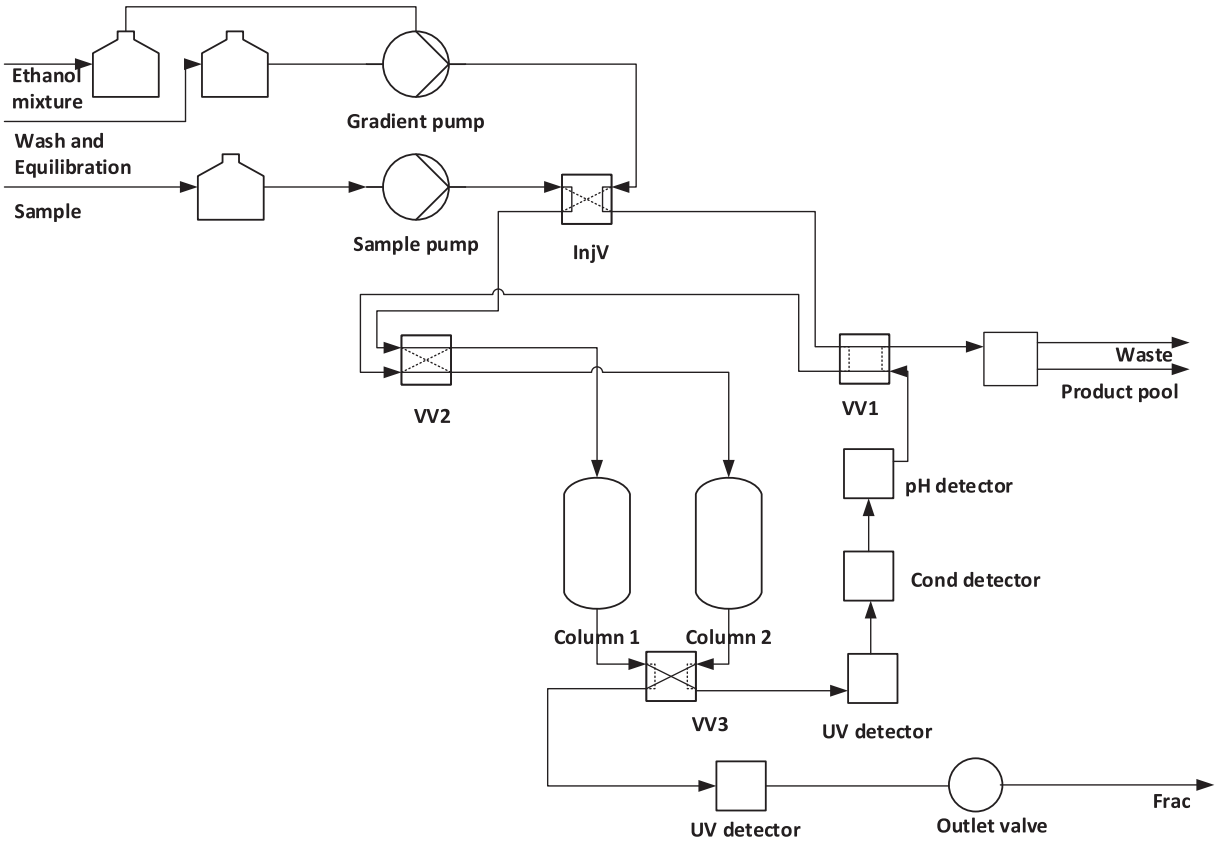

Fig. 2. CaptureSMB process configuration in chromatography system (Step 1). Continuous line represents active flow path.

Table 1
Lab scale CaptureSMB operating parameters.

Parameter	Value
Start-up time	125 min
Interconnected time	83 min
Batch time	42 min
Interconnected superficial velocity	61 cm/h
Batch velocity	30 cm/h
Elution velocity	100 cm/h
Washing and Equilibration velocity	115 cm/h
Resin	FPX66
Column Volume	3.5 mL (1 cm × 4.5 cm; id × h)

3.5. Analytical methods

Sinapic acid concentration was analyzed by Ultra High-Performance Liquid Chromatography (UHPLC, Ultimate 3000, Thermo Scientific, USA) equipped with a C18 column (Acquity UPCL HSS column 1.8 μm, 2.1 mm x 1000 mm Waters, Milford, USA). The column was maintained at 30 °C with a flow of 0.3 mL/min (isocratic elution 66.7% solvent A). Solvent A is MilliQ water (acidified with 10% ferulic acid) and solvent B is acetonitrile (acidified with 10% ferulic acid). Data acquisition was obtained at 325 nm wavelength.

4. Results and discussion

4.1. CaptureSMB experiments

CaptureSMB experiments were performed in an Äkta Avant system for the capture of sinapic acid. The process was monitored by UV and by fractionation as sinapic acid detection by UV easily exceeded the linearity of the detector at concentration higher than 0.2 g/L. Eight product pools were obtained from the four cycles. Sinapic acid breakthrough in column 1, was measured at the end of the run (Fig. 3a), where a breakthrough of around 50% was achieved. The average concentration of sinapic acid in the pools was 3.58 ± 0.22 g/L, therefore the product was concentrated 3.2 times.

Breakthrough of sinapic acid at the exit of the second column (Fig. 3b) during the interconnected phase, is observed and not desirable as product is consequently lost. Product breakthrough continues during the batch phase, when column 1 is being eluted and regenerated and column two is loaded with a lower flowrate. The observed breakthrough is minimum and does not exceed 1% in each cycle, and therefore did not significantly affect sinapic acid recovery yield.

The process mass balance was evaluated (mass balance error of 6%) and the performance indicators, such as, yield, productivity, buffer consumption and resin capacity utilization were calculated (Table 3) and compared with semi-continuous CaptureSMB modelling results. In addition, these results were compared with batch operation at lab scale.

It can be seen in Table 3 that the yield predicted by the simulation of

Table 2
FPX66 resin characteristics.

Resin	Matrix	Particle size (mm)	Surface area (m^2/g)/capacity	Pore diameter (nm)	Density (g/mL)
FPX66	Macroeticular aromatic polymer	0.600–0.750	≥700	25	1.025

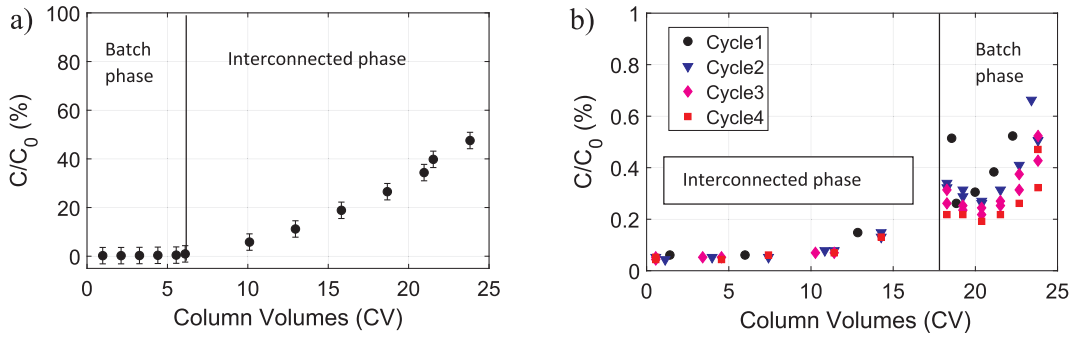

Fig. 3. (a) Sinapic acid breakthrough in column 1, (b) Sinapic acid concentration at the exit of column 2 during interconnected and batch phase in four cycles.

Table 3
Performance comparison between CaptureSMB (experimental and simulation) & batch simulation results.

	CaptureSMB		Batch	Units
	Exp	Simulation	Simulation	
Flow rate	Qic 0.8 Qb 0.4		0.8	mL/min
Yield	95	96	98	%
Productivity	8.8	9.0	6.7	$g/L_R/h$
Buffer consumption	0.7	0.7	1.5	L/g
Capacity utilization	60	62	30	%
Product concentration	3.6	3.7	1.7	g/L

the CaptureSMB process is slightly higher than the one obtained experimentally, however this difference could be attributed to experimental error. The missing sinapic acid might have been lost during the washing step, as observed with the model, where the loss is around 4%.

Comparison between batch and CaptureSMB process was done using the same resin volume. This means that in the CaptureSMB process, the two columns connected have the same total volume as one batch column, and the superficial velocity of the batch process corresponds to the interconnected phase velocity of the CaptureSMB. The results of one single column (batch operation) showed much lower resin capacity utilization due to the limited feed loading. This because the column is loaded just before 4% product breakthrough while in the CaptureSMB the loading reached almost 50% breakthrough. Consequently, higher buffer consumption and lower productivity are observed compared to the semi-continuous process.

It is important to note that the velocities and parameters used in the experiments were pre-estimations and were not optimized. Optimization of both processes is shown in Section 4.2 Batch and CaptureSMB industrial scale optimization.

The previous results validated the CaptureSMB model previously described, and the batch and semi-continuous model were used to perform an industrial-scale process optimization, with the objective of maximizing the productivity. The following sections explain the optimization results.

4.2. Batch and CaptureSMB industrial scale optimization

4.2.1. Batch optimization

For batch adsorption analysis, a column of 1 m internal diameter and three different column lengths, 3 m, 6 m, and 12 m, were simulated. Mechanical resistance of resin FPX66 goes up to 224 kPa/m with a maximum service superficial velocity of 223.0 m/h at 27 °C. The lower velocity limit was set to 2.4 m/h and the upper limit to 205 m/h. Batch optimization was performed to identify the optimum velocity that maximizes productivity without compromising yield (> 97%) and without exceeding maximum pressure drop, having as an additional constraint at least 70% of resin utilization. The superficial velocity for elution/regeneration was set to 80 m/h. As the elution is done with 70% ethanol, the column was also regenerated.

A Pareto chart of resin utilization versus productivity for the batch process is shown in Fig. 4a, for different column lengths. In all data points, the yield condition was accomplished. Fig. 4a shows that higher resin utilization can be reached at any column length but this might decrease productivity, because the points that are closer to 100% resin utilization are the ones that correspond to lower velocities and consequently higher residence time [42]. From Fig. 4a, one can notice that the resin utilization constraint can be accomplished with any column height, and that similar productivity values are also obtained as the curves are almost overlapped at higher than 70% resin utilization.

The highest productivity achieved for a 97% yield (at 4% breakthrough) was found with the shortest column, 10.4 g/L/h, corresponding to resin utilization of 35.5%, which is lower than the desired value of 70%.

It is known that there is a residence time that maximizes

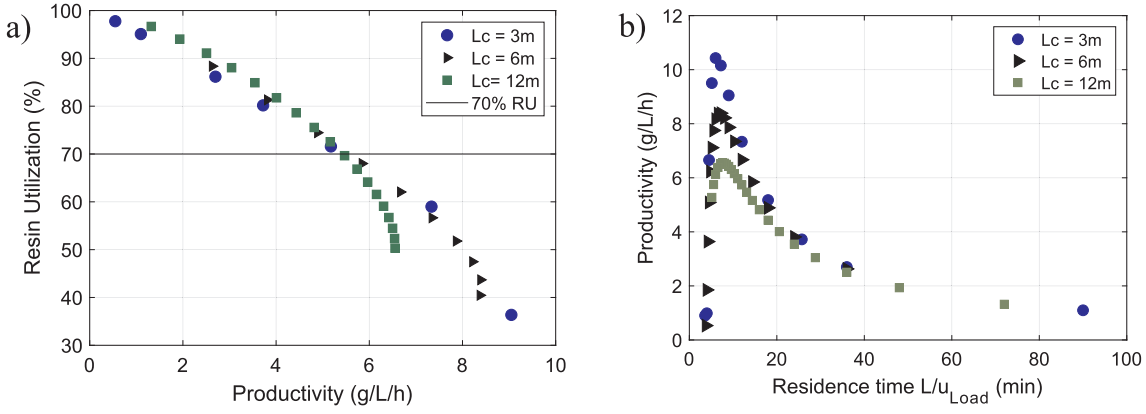

Fig. 4. (a) Resin Utilization vs Productivity in batch process. (b) Productivity vs Residence time.

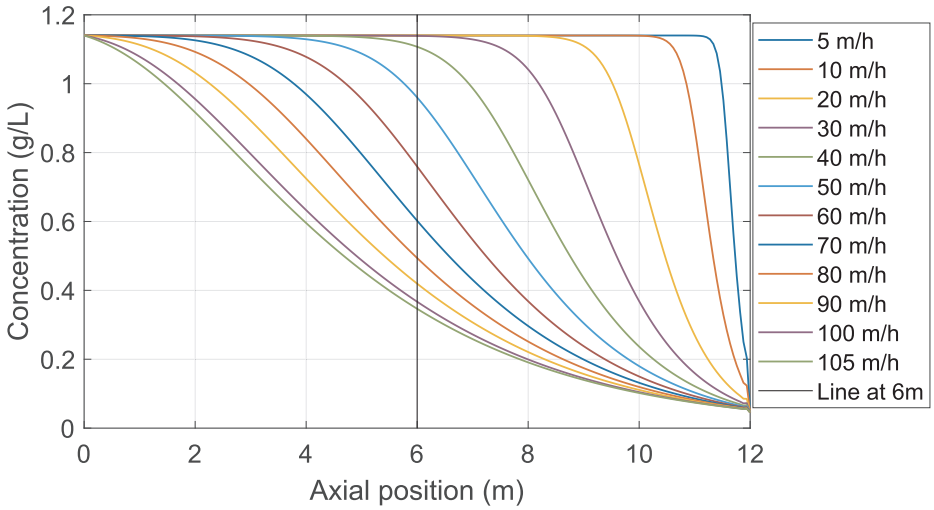

Fig. 5. Product concentration profile inside the column at 4% breakthrough at different superficial velocities.

productivity in a batch process, independently of column length [37], which in this case is around 10 min. The peak height in Fig. 4b, changes with column length because the superficial velocity for wash, elution and re-equilibration was set to 80 m/h, which makes the duration of these steps be different with column length as they are based on column volumes. As the column height increases, higher volumes and more time is required in order to complete this task. This consequently reduces the maximum productivity values for longer columns. It is clear that a batch process can achieve high productivity but inevitably at expense of resin capacity utilization and vice versa, higher resin utilization with lower productivity.

Operating the 12 m column at 50 m/h, the 6 m column at 22 m/h and the 3 m column at 10 m/h results in a process productivity of 5.1 ± 0.2 g/L_R/h, while satisfying both constraints of at least 70% resin utilization and > 97% yield. The dimension of the columns will be therefore determined by the feed stream volume.

The use of a semi-continuous operation might increase the resin capacity utilization and productivity as observed in the CaptureSMB experiments. The following section presents the optimization of the CaptureSMB process.

4.2.2. CaptureSMB optimization

An initial estimate of the loading velocity can be done by using the overall mass balance of sinapic acid (at t*) assuming 100% resin utilization and 100% yield in column 1.

$$Q_{ic}\cdot C_f\cdot t_{ic} + Q_b\cdot C_f\cdot t_b = Q_{rr}\cdot C\cdot t_b \tag{17}$$

where Q_{ic}, Q_b, Q_{rr} are the interconnected, batch and regeneration flow rates (m^3/h), C_f is the product feed concentration (g/L). C is the product concentration at the exit of column 1, and $t_b$and t_{ic} are, respectively, the batch time and interconnected time (s).

With the assumption of 100% resin utilization, the right-hand side of Eq. (17) can be calculated with the isotherm, Eq. (4) and the resin volume. Assuming that the interconnected time is zero, Eq. (17) becomes:

$$Q_b\cdot C_f\cdot t_b = q_{SA,C_f}\cdot V_c\cdot(1-\varepsilon_b) \tag{18}$$

$$A\cdot u_b\cdot C_f\cdot t_b = q_{SA,C_f}\cdot A\cdot L\cdot(1-\varepsilon_b) \tag{19}$$

where A is the cross-sectional area (m^2) and L the column length (m), q_{SA,C_f} is the resin adsorption capacity at feed concentration, (g/L_R).The batch time(t_b) is then equal to the regeneration time, which is defined with the elution protocol and flow rate.

$$t_b = t_{wash} + t_{elution} + t_{cip} + t_{equilibration} \tag{20}$$

$$t_b = \frac{CVrr\cdot V_c}{Q_{rr}} = \frac{CV_{rr}\cdot A\cdot L}{A\cdot u_{rr}} \tag{21}$$

Combining Eq. (21) with (19), a maximum superficial velocity for the batch time can be estimated:

$$u_b^{max} = \frac{q_{SA,C_f}\cdot(1-\varepsilon_b)\cdot u_{rr}}{C_f\cdot CV_{rr}} \tag{22}$$

where CV_{rr} are the number of column volumes needed for washing, elution and regeneration. Note that equation (22) is a function of the feed concentration and the elution/regeneration velocity (u_{rr}). The elution velocity (u_{rr}) is independent of the column size and it was set to 80 m/h. As t_b scales with column length, the maximum batch velocity is 205 m/h. The pressure drop calculated at this velocity is still lower than the mechanical resistance of resin FPX66, for the longest column.

Eq. (17) indicates that the amount of sinapic acid captured in the system (both columns in batch and interconnected phase) should be lower or equal to the maximum capacity assuming that sinapic acid is not lost at the exit of column 2 during the interconnected and batch phase. This amount is equal to the product between the feed concentration, batch time and maximum flow rate, as expressed in Eq. (23).

$$A\cdot u_{ic}\cdot C_f\cdot t_{ic} + A\cdot u_b\cdot C_f\cdot t_b = A\cdot u_b^{max}\cdot C_f\cdot t_b \tag{23}$$

$$u_{ic}\cdot t_{ic} + u_b\cdot t_b = u_b^{max}\cdot t_b \tag{24}$$

Assuming that t_{ic} is equal to t_b and that the batch and interconnected velocities are similar, the resulting velocity would be half of the maximum loading velocity (u_b^{max}). If u_{ic} and u_b are lower than u_b^{max}, it is clear that the interconnected time would always be higher than the batch time. With this analysis it is not possible to identify the upper limit of the interconnected superficial velocity or interconnected time. This is because it was assumed 100% resin capacity utilization, which might not be true. Nevertheless, an indication could be made if the length of the mass transfer zone is known. Using the model, the liquid concentration inside the column can be estimated at different superficial velocities up to 4% breakthrough. The results for a system with 6 m columns (12 m both columns connected) are shown in Fig. 5.

As can be seen (Fig. 5), higher velocities shallow the concentration profiles up to a point where the velocity is so high that will achieve the 4% breakthrough in a very short time, resulting in an unrealistic interconnected phase. Using a 6 m column system, interconnected velocities higher than 100 m/h would lead to lower resin utilization, and depending on the selected interconnected time, it might also affect yield.

Even though, the aforementioned analysis can help to identify the

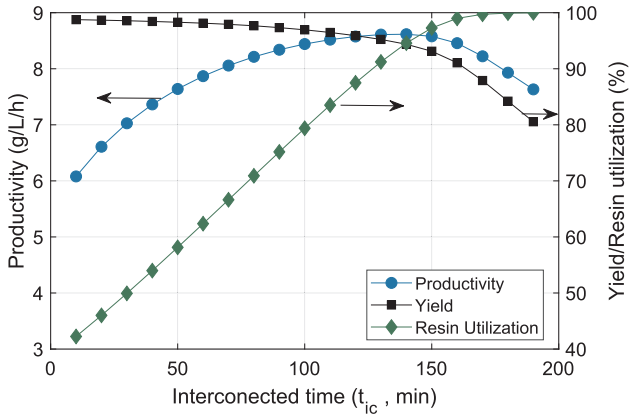

Fig. 6. Productivity, Yield and Resin utilization vs interconnected time. CaptureSMB L_c = 6 m, u_{ic} = 80 m/h u_b = 40 m/h.

velocity boundaries in the CaptureSMB process, there is still one more variable to be optimized, the interconnected time.

Optimizing the interconnected time is not an easy task, as a relatively short interconnected time might lead to lower resin utilization, while a long interconnected time can compromise yield. Because of the breakthrough in the second column, thus causing product loss.

Fig. 6 shows the relationship between productivity, yield and resin utilization (y axis) versus the interconnected time. Longer interconnected time benefits resin utilization but decreases the yield. It can also be seen that productivity increases with longer interconnected times due to the increase of resin utilization, however it starts decreasing when the yield is reduced due to product loss. Longer interconnected time will allow the product to reach the end of the second column and breakthrough. Product loss continues during the disconnected phase as the second column is continuously loaded with the feed at a lower flow rate. Therefore, in order not to compromise yield and still improve resin utilization, a trade-off between interconnected velocity and time should be found. In the case of the CaptureSMB system using 6 m columns, the maximum productivity obtained is around 8.5 g/L_R/h by operating the system at 80 m/h during the interconnected phase for 105 min. Even though the CaptureSMB system could be operated at lower interconnected velocities (Fig. 5) to increase resin utilization, it will also require that the columns are connected for a longer period, and this might reduce productivity.

Similarly to the 1-column process (batch process), the maximum achievable productivity decreases if the column length is higher, due to the much longer time needed to complete the elution and regeneration of the columns. The productivity values can be found in Table 4, where the highest is obtained with the CaptureSMB system with shortest columns. The opposite happens with resin utilization, which improves with higher column lengths. This might be attributed to mass transfer limitation, as the breakthrough curve of sinapic acid is relatively shallow which also allows the product to reach the exit of the second column relatively fast, which becomes more evident if the CaptureSMB system is short. The optimized parameters for the batch (packed bed) and semi-continuous (CaptureSMB) process are shown in Table 4. In all evaluated column lengths, the productivity and resin utilization values are higher than the ones obtained for batch operation. The highest productivity value, accomplishing the yield condition of 97%, was found in the shortest column system (L_c = 3 m) with a resin utilization of 72%. Increasing column size in the CaptureSMB process improves resin utilization, but as with the batch process, the productivity is reduced due to the increasing time of elution and regeneration steps at the same superficial velocity of 80 m/h.

Table 4
Optimized parameters for batch (packed bed) and semi-continuous (CaptureSMB) processes to recover sinapic acid.

	Batch process	Capture SMB 1	Capture SMB 2	Capture SMB3
Column length (m)	3/6/12	3	6	12
Interconnected time/Time switch (min)	533*	85/119	105/173	120/255
Interconnected velocity, u_{ic} (m/h)	10**/ 22**/50**	50	80	150
Batch velocity, u_b (m/h)	N/A	10	40	68
Yield (%)	98	97	97	97
Productivity (g/L/h)	5.18	10.3	8.7	7.2
Resin utilization (%)	71	72	82	92
Product concentration (g/L)	3.8	3.8	4.2	5.1
Buffer consumption (L/g)	0.5	0.5	0.4	0.4

* Batch cycle time.
** Adsorption velocity.

5. Conclusions

This work demonstrates that the semi-continuous CaptureSMB process outperforms batch packed-bed operation for the recovery of sinapic acid, showing higher productivity, resin capacity utilization and lower buffer consumption without compromising yield. The obtained equilibrium information in combination with mechanistic models is a powerful tool to optimize process parameters, both in batch and semi-continuous mode. In addition, the validated model can be used as a predictive tool to evaluate performances at different column sizes. This methodology could be extended to recover similar molecules from voluminous food side streams using similar adsorbents, as it allows operating the purification process continuously, which is desired in the food sector as most of its operation is performed in continuous mode.

CRediT authorship contribution statement

Mónica Moreno-González: Writing - original draft, Methodology, Software, Formal analysis, Validation, Investigation, Visualization, Project administration. **Daphne Keulen:** Methodology, Software, Visualization, Formal analysis. **Joaquín Gomis-Fons:** Methodology, Software, Formal analysis, Writing - review & editing. **Gustavo Lopez Gomez:** Methodology, Formal analysis, Writing - review & editing. **Bernt Nilsson:** Software, Writing - review & editing. **Marcel Ottens:** Conceptualization, Writing - review & editing, Supervision, Project administration, Funding acquisition.

Declaration of Competing Interest

The authors declare that they have no known competing financial interests or personal relationships that could have appeared to influence the work reported in this paper.

Acknowledgments

This work was supported by the ISPT (Institute of Sustainable Process Technology) under the project CM-20-07 in Adsorption of non-volatiles from food products. Thank you to the industrial partners DSM, Unilever, Friesland Campina and Royal Cosun for their valuable input throughout the project.

Appendix A. Supplementary material

Supplementary data to this article can be found online at https://doi.org/10.1016/j.seppur.2020.117403.

References

[1] C.M. Galanakis, Recovery of high added-value components from food wastes: conventional, emerging technologies and commercialized applications, Trends Food Sci. Technol. 26 (2012) 68–87, https://doi.org/10.1016/j.tifs.2012.03.003.

[2] S. Bérot, J.P. Compoint, C. Larré, C. Malabat, J. Guéguen, Large scale purification of rapeseed proteins (*Brassica napus L.*), J. Chromatogr. B 818 (2005) 35–42, https://doi.org/10.1016/j.jchromb.2004.08.001.

[3] J.P. Wanasundara, Proteins of Brassicaceae oilseeds and their potential as a plant protein source, Crit. Rev. Food Sci. Nutr. 51 (2011) 635–677, https://doi.org/10.1080/10408391003749942.

[4] A. Fetzer, T. Herfellner, A. Stäbler, M. Menner, P. Eisner, Influence of process conditions during aqueous protein extraction upon yield from pre-pressed and cold-pressed rapeseed press cake, Ind. Crop Prod. 112 (2018) 236–246, https://doi.org/10.1016/j.indcrop.2017.12.011.

[5] G. Ganetsos, P. Barker, Developments in large-scale batch chromatography, in: G. Ganetsos, P. Barker (Eds.) Preparative and production scale chromatography, 1992, pp. 3–10.

[6] F. Steinebach, T. Muller-Spath, M. Morbidelli, Continuous counter-current chromatography for capture and polishing steps in biopharmaceutical production, Biotechnol. J. 11 (2016) 1126–1141, https://doi.org/10.1002/biot.201500354.

[7] J.P.S. Aniceto, C.M. Silva, Simulated Moving Bed Strategies and Designs: From Established Systems to the Latest Developments, Sep. Purif. Rev. 44 (2015) 41–73, https://doi.org/10.1080/15422119.2013.851087.

[8] M. Mazzotti, G. Storti, M. Morbidelli, Optimal operation of simulated moving bed units for nonlinear chromatographic separations, J. Chromatogr. A 769 (1997) 3–24, https://doi.org/10.1016/S0021-9673(97)00048-4.

[9] A. Rajendran, G. Paredes, M. Mazzotti, Simulated moving bed chromatography for the separation of enantiomers, J. Chromatogr. A 1216 (2009) 709–738, https://doi.org/10.1016/j.chroma.2008.10.075.

[10] A.E. Rodrigues, C. Pereira, M. Minceva, L.S. Pais, A.M. Ribeiro, A. Ribeiro, M. Silva, N. Graça, J.C. Santos, Simulated Moving Bed Technology, first ed., Butterworth-Heinemann, Oxford, 2015.

[11] C. Berg, Hypersorption design - modern advancements, Chem. Eng. Prog. 47 (1951) 585–590.

[12] G. Ganetsos, P.E. Barker, Semicontinuous countercurrent chromatography refiners, in: G. Ganetsos, P.E. Barker (Eds.), Preparative and Production Scale Chromatography, Marcel Dekker Inc, New York, 1993, pp. 233–255.

[13] J.A. Johnson, R.G. Kabza, Sorbex: industrial scale adsorptive separation, in: G. Ganetsos, P.E. Barker (Eds.), Preparative and Production Scale Chromatography, Malcel Dekker Inc, New York, 1993, pp. 257–271.

[14] M. Juza, M. Mazzotti, M. Morbidelli, Simulated moving-bed chromatography and its application to chirotechnology, Trends Biotechnol. 18 (2000) 108–118, https://doi.org/10.1016/S0167-7799(99)01419-5.

[15] R. Godawat, K. Brower, S. Jain, K. Konstantinov, F. Riske, V. Warikoo, Periodic counter-current chromatography – design and operational considerations for integrated and continuous purification of proteins, Biotechnol. J. 7 (2012) 1496–1508.

[16] V. Warikoo, R. Godawat, K. Brower, S. Jain, D. Cummings, E. Simons, T. Johnson, J. Walther, M. Yu, B. Wright, J. McLarty, K.P. Karey, C. Hwang, W. Zhou, F. Riske, K. Konstantinov, Integrated continuous production of recombinant therapeutic proteins, Biotechnol. Bioeng. 109 (2012) 3018–3029, https://doi.org/10.1002/bit.24584.

[17] C.K.S. Ng, F. Rousset, E. Valery, D.G. Bracewell, E. Sorensen, Design of high productivity sequential multi-column chromatography for antibody capture, Food Bioprod. Process. 92 (2014) 233–241, https://doi.org/10.1016/j.fbp.2013.10.003.

[18] O. Ludemann-Hombourger, R.M. Nicoud, M. Bailly, The "VARICOL" process: a New multicolumn continuous chromatographic process, Sep. Sci. Technol. 35 (2000) 1829–1862, https://doi.org/10.1081/SS-100100622.

[19] M. Krättli, T. Müller-Späth, M. Morbidelli, Multifraction separation in countercurrent chromatography (MCSGP), Biotechnol. Bioeng. 110 (2013) 2436–2444, https://doi.org/10.1002/bit.24901.

[20] L. Aumann, M. Morbidelli, A continuous multicolumn countercurrent solvent gradient purification (MCSGP) process, Biotechnol. Bioeng. 98 (2007) 1043–1055, https://doi.org/10.1002/bit.21527.

[21] F. Janakievski, O. Glagovskaia, K. De Silva, Simulated moving bed chromatography in food processing, in: K. Knoerzer, P. Juliano, G. Smithers (Eds.), Innovative Food Processing Technologies, Woodhead Publishing, 2016, pp. 133–149.

[22] D. Costesso, G. Rearick, M.J.Z. Kearney, Improved simulated moving bed process for purifying sugar solutions, Zuckerindustrie 125 (2000) 333–335.

[23] Y. Xie, C.Y. Chin, D.S.C. Phelps, C.-H. Lee, K.B. Lee, S. Mun, N.-H.-L. Wang, A Five-Zone Simulated Moving Bed for the Isolation of Six Sugars from Biomass Hydrolyzate, Ind. Eng. Chem. Res. 44 (2005) 9904–9920, https://doi.org/10.1021/ie050403d.

[24] E.J. Freydell, Y. Bulsink, S. van Hateren, L. van der Wielen, M. Eppink, M. Ottens, Size-exclusion simulated moving bed chromatographic protein refolding, Chem. Eng. Sci. 65 (2010) 4701–4713, https://doi.org/10.1016/j.ces.2010.05.023.

[25] M. Ottens, J. Houwing, S.H. Van Hateren, T. Van Baalen, L.A.M. Van der Wielen, Multi-component fractionation in SMB chromatography for the purification of active fractions from protein hydrolysates, Food Bioprod. Process. 84 (2006) 59–71, https://doi.org/10.1205/fbp.05185.

[26] H.-G. Nam, C. Park, S.-H. Jo, Y.-W. Suh, S. Mun, Continuous separation of succinic acid and lactic acid by using a three-zone simulated moving bed process packed with Amberchrom-CG300C, Process Biochem. 47 (2012) 2418–2426, https://doi.org/10.1016/j.procbio.2012.09.027.

[27] D.C.S. Azevedo, A.E. Rodrigues, Fructose–glucose separation in a SMB pilot unit: modeling, simulation, design, and operation, AlChE J. 47 (2001) 2042–2051.

[28] K. Hashimoto, Models for the separation of glucose/fructose mixture using a simulated moving-bed adsorber, J. Chem. Eng. Jpn. 16 (1983) 400.

[29] K. Hashimoto, Continuous separation of glucose-salts mixture with nonlinear and linear adsorption isotherms by using a simulated moving-bed adsorber, J. Chem. Eng. Jpn. 20 (1987) 405.

[30] T. Müller-Späth, M. Morbidelli, Continuous chromatography in biomanufacturing, in: G. Subramanian (Ed.), Continuous Biomanufacturing - Innovative Technologies and Methods, Wiley-VCH, 2017, pp. 393–422.

[31] M. Angarita, T. Müller-Späth, D. Baur, R. Lievrouw, G. Lissens, M. Morbidelli, Twin-column CaptureSMB: a novel cyclic process for protein A affinity chromatography, J. Chromatogr. A 1389 (2015) 85–95, https://doi.org/10.1016/j.chroma.2015.02.046.

[32] D. Baur, M. Angarita, T. Müller-Späth, M. Morbidelli, Optimal model-based design of the twin-column CaptureSMB process improves capacity utilization and productivity in protein A affinity capture, Biotechnol. J. 11 (2016) 135–145, https://doi.org/10.1002/biot.201500223.

[33] M. Moreno-González, V. Girish, D. Keulen, H. Wijngaard, X. Lauteslager, G. Ferreira, M. Ottens, Recovery of sinapic acid from canola/rapeseed meal extracts by adsorption, Food Bioprod. Process. 120 (2020) 69–79, https://doi.org/10.1016/j.fbp.2019.12.002.

[34] J.M. Bell, Nutrients and toxicants in rapeseed meal: a review, J. Anim. Sci. 58 (1984) 996–1010, https://doi.org/10.2527/jas1984.584996x.

[35] N. Nićiforović, H. Abramovič, Sinapic acid and its derivatives: natural sources and bioactivity, Compr. Rev. Food Sci. Food Saf. 13 (2014) 34–51, https://doi.org/10.1111/1541-4337.12041.

[36] A. Felinger, G. Guiochon, Comparison of the kinetic models of linear chromatography, Chromatographia 60 (2004) S175–S180.

[37] G. Carta, A. Jungbauer, Protein Chromatography: Process Development and Scale-up, John Wiley & Sons, 2010.

[38] M. Silva, L. Castellanos, M. Ottens, Capture and purification of polyphenols using functionalized hydrophobic resins, Ind. Eng. Chem. Res. 57 (2018) 5359–5369, https://doi.org/10.1021/acs.iecr.7b05071.

[39] T. Muller-Spath L. Aumann, G. Strohlein, M. Bavand, N. Ulmer, Chromatographic process for enrichment and isolation, in: ChromaCon AG, Patent No. US9073970B2, United States, 2014.

[40] N. Andersson, A. Löfgren, M. Olofsson, A. Sellberg, B. Nilsson, P. Tiainen, Design and control of integrated chromatography column sequences, Biotechnol. Progr. 33 (2017) 923–930, https://doi.org/10.1002/btpr.2434.

[41] J. Gomis-Fons, A. Löfgren, N. Andersson, B. Nilsson, L. Berghard, S. Wood, Integration of a complete downstream process for the automated lab-scale production of a recombinant protein, J. Biotechnol. 301 (2019) 45–51, https://doi.org/10.1016/j.jbiotec.2019.05.013.

[42] J. Gomis-Fons, N. Andersson, B. Nilsson, Optimization study on periodic counter-current chromatography integrated in a monoclonal antibody downstream process, J. Chromatogr. A 1621 (2020) 461055, https://doi.org/10.1016/j.chroma.2020.461055.

[43] T. McIlvaine, A buffer solution for colorimetric comparison, J. Biol. Chem. 49 (1921) 183–186.